Color-Tunable Organic Microcavity Laser Array Using Distributed Feedback

Giuseppe Strangi,* Valentin Barna, Roberto Caputo, Antonio De Luca, Carlo Versace, Nicola Scaramuzza, Cesare Umeton, and Roberto Bartolino

LICRYL-INFM and Center of Excellence CEMIF.CAL, Department of Physics, University of Calabria, I-87036 Rende (CS), Italy

Gabriel Noam Price

Department of Physics and FLCMRC (Ferroelectric Liquid Crystal Materials Research Center), University of Colorado, Boulder, Colorado 80309-0390, USA

(Received 30 August 2004; published 17 February 2005)

Distributed feedback microstructures play a fundamental role in confining and manipulating light to obtain lasing in media with gain. Here, we present an innovative array of organic, color-tunable microlasers which are intrinsically phase locked. Dye-doped helixed liquid crystals were embedded within periodic, polymeric microchannels sculptured by light through a single-step process. The helical superstructure was oriented along the microchannels; the lasing was observed along the same direction at the red edge of the stop band. Several physical and technological advantages arise from this engineered heterostructure: a high quality factor of the cavity, ultralow lasing threshold, and thermal and electric control of the lasing wavelength and emission intensity. This level of integration of guest-host systems, embedded in artificially patterned small sized structures, might lead to new photonic chip architectures.

DOI: 10.1103/PhysRevLett.94.063903 PACS numbers: 42.70.Qs, 42.70.Df

Photonic crystals that strongly localize light are finding applications in many areas of physics and engineering, including coherent electrophoton interactions [1], photonic chips [2], nonlinear optics [3], low-threshold laser [4], and quantum information processing [5]. Photonic crystals are periodic dielectric structures that can selectively reflect light for any direction of propagation in specific wavelength ranges. This property, which can be used to confine, manipulate, and guide photons, should allow the creation of all-optical integrated circuits. In analogy with the energy gap in semiconductors, where a forbidden window opens up between the valence and the conduction bands, a dielectric periodic structure shows a stop band in the spectrum of propagating electromagnetic modes, known as the photonic band gap (PBG). In PBG microstructures light can be confined and manipulated by engineering ideal distributed feedback (DFB) microresonators. Confinement of light to small volumes has important implications for optical emission properties: it changes the probability of spontaneous emission from atoms, allowing both enhancement and inhibition [6,7]. Chiral liquid crystals (LCs) possess a helical superstructure which provides a 1D spatial modulation of the refractive index giving rise to Bragg selective reflection for circularly polarized light having the same handedness as the LC structure. Circular Bragg reflection occurs between wavelengths $\lambda_1 = pn_o$ and $\lambda_2 = pn_e$, where n_o and n_e are the ordinary and extraordinary refractive indices of the locally uniaxial structure, and p is the pitch of the helical structure. The optical reflection band is centered at $\lambda_c = pn_{\mathrm{av}}$ with a bandwidth $\Delta\lambda = (n_e - n_o)p$, where n_{av} is the average refractive index.

In a medium with gain, such as a chiral LC doped with fluorescent guest molecules, a photonic band gap affects the emission spectrum. Within the band gap, where the wave is evanescent and decays exponentially, the spontaneous emission is suppressed. This can be explained by taking into account that the photonic density of states (DOS) vanishes in large periodic structures and the rate of the spontaneous emission is proportional to the DOS [8]. The DOS diverges as the band edge is approached, owing to the fact that the group velocity approaches zero in proximity of the edges, and the resulting long dwell time of the emitted photons strongly supports stimulated emission [9].

Kogelnik and Shank [10] were the first to report laser action in periodic DFB structures which do not utilize conventional cavity mirrors but provide optical feedback via backward Bragg scattering. Lasing has been demonstrated in dye-doped cholesteric liquid crystals [11], liquid crystals in polymer networks [12–14], and also ferroelectric liquid crystals [15]. Here we report the fabrication of color-tunable, DFB microcavity lasers with a high ratio between the quality factor Q of the cavity and its volume V, the Purcell number [16]. The optical microcavities were obtained by embedding dye-doped helixed liquid crystals in holographically patterned polymeric microchannels (Fig. 1). The orientation of the LC helix axis along the microchannels offers several physical advantages: increase of the cavity length and thus the number of periods, small modal volume, directional control, improvement of the liquid crystal orientational order parameter, and wavelength tunability. The distributed feedback needed to obtain laser oscillations in the case of a small refractive index modulation requires thousands of periods in order to behave as an optical cavity with a quite high quality factor, $Q \sim 280$ [17]. The presented geometry allows obtaining a number of periods which is about 2 orders of magnitude larger than conventional systems because it exploits the

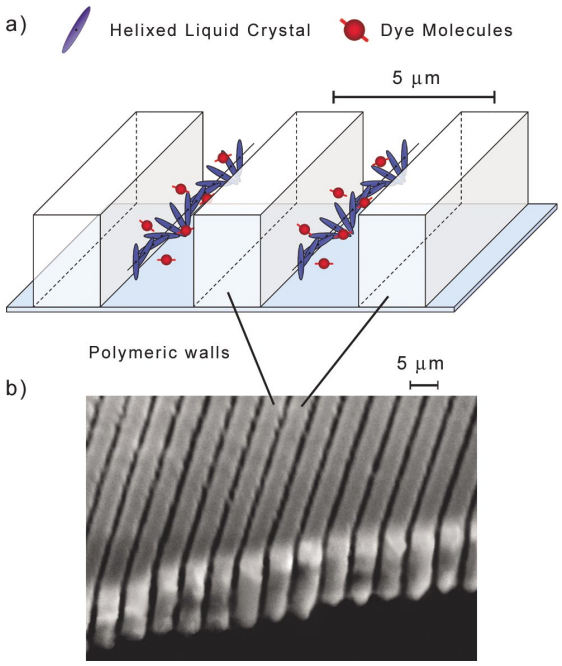

FIG. 1 (color). Spatial geometry of photopatterned organic microcavities. (a) Diagram of the periodic microstructure hosting the dye-doped helixed liquid crystal oriented parallel to the polymer walls. (b) Scanning electron microscopy image of the presented structure shows a very sharp morphology. Spatial periodicity of the structure is $\sim 5\ \mu$m with a microcavity width of $\sim 1.5\ \mu$m.

entire length of the microchannel in a waveguide regime instead of the sample thickness. In this way, each microchannel becomes an optical mirrorless microcavity with a very small volume V of only a few cubic micrometers. This results in a remarkable Purcell number (~ 3) which is very desirable since it enhances the factor of spontaneous emission and severely reduces the threshold of laser emission. The fabricated structure is sketched in Fig. 1(a). Between two indium tin oxide (ITO) coated glass plates separated by 13.5 μm thick mylar spacers, we have confined a mixture of 29.9 wt % BL088 cholesteric liquid crystal (Merck), 69.3 wt % of NOA-61 monomer (Norland), 0.7 wt % of Irgacure 2100 and Darocur 1173 photoinitiators (1:1 wt %, Ciba Specialty Chemicals), and 0.09 wt % of pyrromethene dye (Exciton). The sample was then irradiated for 17.0 min with the interference pattern produced by two UV laser beams ($\lambda = 351$ nm, from an Innova-90C source, Coherent), at an intensity of 1.05 mW/cm^2 each.

A series of side-by-side microchannels with a very sharp morphology was produced by a photopolymerization process which was locally induced by the sinusoidally modulated light intensity [Fig. 1(b)]. The angle θ between the two interfering beams ($\sim 2°$) was used to select a structure period Λ of 5 μm, according to the relation $\Lambda = \lambda/2\sin\theta$, where λ is the irradiation wavelength. However, this periodicity can range from 200 nm to some micrometers. By means of a miniature oven (CaLCTec S.r.l.) it was possible to maintain the entire mixture at a fixed temperature ($\sim 90\,°$C), thus allowing the liquid-crystalline component to remain in the isotropic phase during the whole irradiation process. This approach increases the mass diffusion rate and prevents the formation of liquid crystal droplets encapsulated in the polymer as evidenced by the very low scattering exhibited by the sample. It is worth noting that the diffusion coefficient of the liquid crystal molecules is highly anisotropic due to their rodlike shape: diffusing from the polymer network, the molecules find an "easy way" aligning perpendicular to the polymeric walls. By slowly cooling the sample to room temperature ($-0.5\,°$C min^{-1}) a self-organization process occurs owing to the isotropic-chiral liquid crystal phase transition. The system tends to minimize its free energy by orienting the liquid crystal helices, on average, along the microchannels. In fact, the light polarization orientation which experiences the lower refractive index was experimentally measured by optical techniques (photopolarimetry and tilting optical compensator) indicating the orientation of the helix axis. At the end of the whole process an almost complete phase separation was obtained, giving rise to helixed liquid crystal channels periodically separated by polymer walls.

The sample was optically pumped with 3 ns pulses produced by a frequency-doubled (532 nm) Nd-doped:yttrium aluminum garnet (Nd:YAG) laser (NewWave, Tempest 20). The pump beam was focused onto the sample with a cylindrical lens ($f = 100$ mm) producing an elliptical profile (with a short axis of approximately 50 μm). The long axis of this beam profile was oriented perpendicularly to the microchannels orientation so that several channels were simultaneously optically pumped. The PBG structure of the self-organized liquid crystal severely modified the fluorescence spectrum of the dye molecules: at low pump energies a dip in the emission occurred at the position of stop band. By increasing the pump energy above a given threshold value, highly directional laser action was observed along the microchannels at the low-energy edge of the stop band, where the photonic density of the states diverges and the lasing is expected [Fig. 2(a)]. Just above the threshold value and at room temperature the average lifetime of the gain medium is of several weeks. Anyway, dye photodegradation has been observed for pumping energy far above the threshold value (tens of μJ/pulse) which strongly reduces the lifetime (few minutes).

The photonic density of states ρ is defined as the inverse slope of the dispersion relation [8]:

$$\rho = \left| \frac{d}{d\omega} \mathrm{Re}(K) \right|. \tag{1}$$

In an isotropic medium with refractive index n, the DOS is $\rho_{\mathrm{iso}} = n/c$, where c is the speed of light *in vacuo*. By considering a birefringent chiral liquid crystal confined in long microcavities (LMC) where effects due to multiple reflections at the interfaces can be neglected, the DOS are calculated as follows:

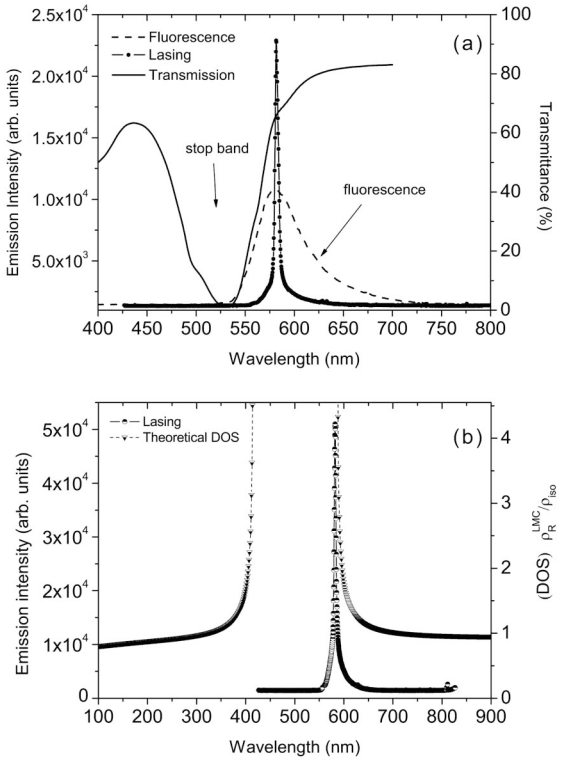

FIG. 2. Lasing spectra. (a) Transmission, fluorescence, and lasing spectra are reported. Highly directional laser action was observed along the microchannels within a limited cone angle (~0.1 rad). (b) The calculated DOS are reported together with the lasing emission.

$$\rho_R^{\mathrm{LMC}} = \frac{1}{p}\left(\frac{d\tilde{k}}{d\tilde{\lambda}}\,\frac{d\tilde{\lambda}}{d\omega}\right), \tag{2}$$

where $\tilde{k} = kp$ and $\tilde{\lambda} = \lambda/(n_{\mathrm{av}}p)$ are the reduced wave number and the reduced wavelength, respectively. By deriving the quantities on the right-hand side of Eq. (2) and by inserting the relative dielectric anisotropy α and the reduced index of refraction $\tilde{n}$,

$$\tilde{n} = 1 + \tilde{\lambda}^2 - (4\tilde{\lambda}^2 + \alpha^2)^{1/2}, \tag{3}$$

one finally obtains the DOS:

$$\rho_R^{\mathrm{LMC}} = \frac{n_{\mathrm{av}}\tilde{n}}{c} - \frac{n_{\mathrm{av}}\tilde{\lambda}^2}{\tilde{n}c}\left(1 - \frac{2}{\sqrt{4\tilde{\lambda}^2 + \alpha^2}}\right). \tag{4}$$

The calculated DOS diverges as the edges of the PBG is approached, matching very well with the experimental spectral position of the lasing emission in microcavities [see Fig. 2(b)]. The lowest lasing threshold measured was 25 nJ/pulse. This value is about an order of magnitude lower than in conventional systems in which optimized materials were used under the same pumping conditions. The laser emissions emerging parallel to the glass plates and along the microchannels direction were captured in a limited cone of ~0.1 rad by using a multichannel charge-coupled device (Jobin-Yvon CP200). The laser emissions were found to be circularly polarized, indicating that distributed feedback mechanisms take place through circular Bragg reflection. The LC microchannel behaves as a miniaturized mirrorless cavity laser, where the emitted laser light propagates in the waveguide defined by the chiroselective liquid-crystalline medium. The most interesting aspect of this lasing system is that optical and geometrical parameters can be modified by applying weak external fields (temperature, electric field, mechanical stress, and optical field), resulting in a direct control of lasing features (wavelength, bandwidth, and emission intensity). In fact, upon varying the temperature of the system the wavelength of laser emission was observed to redshift [Fig. 3(a)] from 580 to 590 nm. This experimental evidence definitely proves that the distributed feedback mechanism, provided by the dielectric tensor modulation of the helixed liquid crystal, is behind the observed effect. It is well known that the period of the helical superstructure, the pitch p, typically changes with increasing temperatures producing an overall displacement of the spectral region where the circular Bragg reflection occurs. Thus, the thermal elongation of the pitch results in a shifting of the stop band edge where the laser actions is expected.

Another striking feature of the presented system is the possibility of controlling the intensity of the lasing emis-

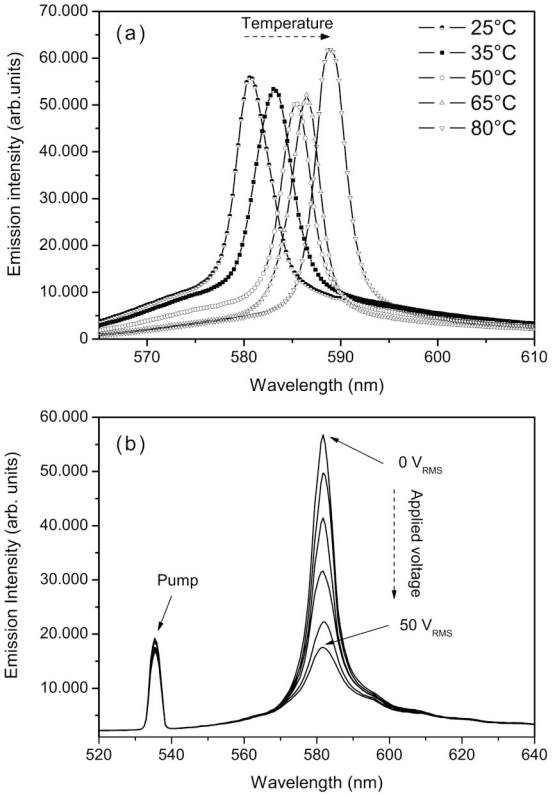

FIG. 3. Temperature and electric field dependence of lasing features. (a) Temperature control of the lasing wavelength (0.2 nm/°C) was obtained by increasing the temperature from 25 °C up to 80 °C. (b) The emission intensity control was achieved by applying an electric field perpendicular to the helical structure, allowing a reversible control of the lasing intensity.

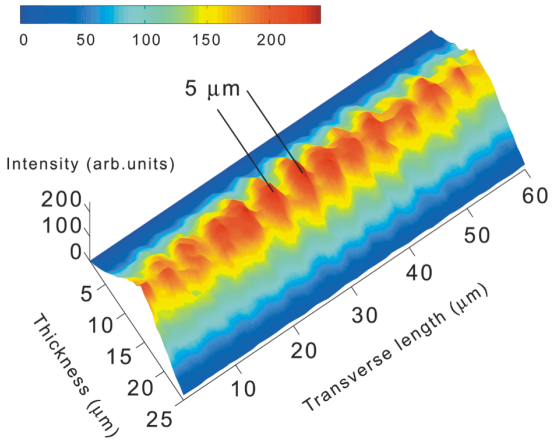

FIG. 4 (color). Spatial distribution of the laser emission emerging from the microcavity array. The image was acquired by scanning in the proximity of the output edge of the cell in a direction perpendicular to the channels. The microlaser array showed a periodicity of $\sim 5\ \mu$m which correlates exactly with the cell geometry.

sion by applying an electric field perpendicular to the helix axis [Fig. 3(b)]. By maintaining a fixed pump energy and varying the amplitude of the applied sinusoidal voltage between 0 and 50 V_{rms} (1 kHz), a fourfold lowering of the emission intensity was observed. This effect provides a unique feature to this system, because it allows a direct control of an important physical parameter by means of an externally induced collective distortion of the LC helices. Under the action of the electric field a local molecular reorientation occurs, which transforms the sinusoidal modulation of the refractive index into a rectangular one producing a severe reduction of the feedback mechanism [18]. In addition to the attenuation of the emission intensity, above a given value of the applied voltage the microcavity laser can be switched off because of a complete unwinding of the helical superstructure which eliminates the distributed feedback.

A spatial distribution analysis of the laser emission intensity was performed in order to have a clearer picture of the presented lasing system. The near-filed emission pattern was acquired by means of a high sensitivity (1390 × 1024 12 bit PixelFlyQE by PCO) charge-coupled device (CCD) imaging camera, and it shows an interesting microlaser array scenario (Fig. 4). A transverse image scan indicates that the spatial periodicity of the array exactly matches the periodicity of the microchannels. Furthermore, the spatial mode characterization emphasizes that elliptic Gaussian beams emerge from the microcavities, acting as astigmatic waveguide resonators. In fact, the locus of the x-y plane where the field is down by a factor $1/e$ from its value on the axis is an ellipse (ellipticity equal to 7.1).

The microlasers of the array are intrinsically phase locked because they are simultaneously stimulated by the same laser pump. Furthermore, tailoring a proper array of electrodes which enables the application of a local electric field would give rise to electrically programmable phase holograms with interesting light polarization properties. An ultralow-threshold color-tunable microlaser array was created by embedding dye-doped helixed liquid crystals in holographically sculptured polymeric microchannels. This level of integration might lead to new photonic chip architectures and devices, such as zero-threshold microlaser, phased array, discrete cavity solitons, filters, and routers.

We acknowledge discussions with Lev M. Blinov and Noel A. Clark. This work was supported by the U.S. National Science Foundation through the "FLCMRC-LICRYL research centers collaborative project" DMR-0302060, and Italian MIUR research project "Piani di Potenziamento della Rete Scientifica e Tecnologica" Cluster No. 26-P4W3.

*Corresponding author.
Electronic address: Strangi@fis.unical.it

[1] G. Khitrova, H. M. Gibbs, F. Jahnke, M. Kira, S. W. Koch, Rev. Mod. Phys. **71**, 1591 (1999).
[2] J. D. Joannopoulos, R. D. Meade, and J. N. Winn, *Photonic Crystals: Moulding the Flow of Light* (Princeton University Press, Princeton, NJ, 1995); S. Noda, K. Tomoda, N. Yamamoto, and A. Churlnan, Science **289**, 604 (2000).
[3] S. Spillane, T. J. Kippenberg, and K. J. Vahala, Nature (London) **415**, 621 (2002).
[4] O. Painter *et al.*, Science **284**, 1819 (1999).
[5] P. Michler *et al.*, Science **290**, 2282 (2000).
[6] E. Yablonovitch, Phys. Rev. Lett. **58**, 2059 (1987).
[7] D. Wiersma, Nature (London) **406**, 132 (2000).
[8] J. Schmidtke and W. Stille, Eur. Phys. J. B **31**, 179 (2003).
[9] J. P. Dowling, M. Scalora, M. J. Bloemer, and C. M. Bowden, J. Appl. Phys. **75**, 1896 (1994).
[10] H. Kogelnik and C. V. Shank, Appl. Phys. Lett. **18**, 152 (1971).
[11] I. P. Il'chishin, E. A. Tikhonov, V. G. Tishchenko, and M. T. Shpak, JETP Lett. **32**, 24 (1980); V. I. Kopp, B. Fan, H. K. M. Vithana, and A. Z. Genack, Opt. Lett. **23**, 1707 (1998); W. Cao, A. Munoz, P. Palffy-Muhoray, and B. Taheri, Nat. Mater. **1**, 111 (2002).
[12] H. Finkelmann, S. T. Kim, A. Munoz, P. Palffy-Muhoray, and B. Taheri, Adv. Mater. **13**, 1069 (2001).
[13] J. Schmidtke, W. Stille, H. Finkelmann, and S. T. Kim, Adv. Mater. **14**, 746 (2002).
[14] P. A. Bermel and M. Warner, Phys. Rev. E **65**, 056614 (2002); P. Cicuta, A. R. Tajbakhsh, and E. M. Terentjev, Phys. Rev. E **65**, 051704 (2002).
[15] M. Ozaki, M. Kasano, D. Ganzke, W. Haase, and K. Yoshino, Adv. Mater. **14**, 306 (2002); G. Price, G. Strangi, A. Klittnick , J. E. Maclennan, and N. A. Clark (unpublished).
[16] E. M. Purcell, Phys. Rev. **69**, 681 (1946).
[17] A. Yariv, *Quantum Electronics* (CBS College Publishing, New York, 1985).
[18] L. M. Blinov and V. G. Chigrinov, *Electrooptic Effects in Liquid Crystal Materials* (Springer-Verlag, New York, 1994).